New insights on planetary companions of GJ 1151

Author: Jordi Blanco Pozo
*Facultat de Física, Universitat de Barcelona, Diagonal 645, 08028 Barcelona, Catalonia, Spain.**

Advisors: Manuel Perger and Carme Jordi i Nebot

Abstract: The LOFAR mission announced the detection of a radio emission coming from the M dwarf GJ 1151 which is consistent with the possible interaction of the star with an Earth-like exoplanet with an orbit of 1 to 5 d. Combining new data from different radial velocity surveys we calculate a new upper limit on the minimum mass of this possible companion at 0.9 $M_\oplus$ to 1.6 $M_\oplus$ for a 1.02 d to 5 d orbit. We also find evidence of a Neptune-like companion with a minimum mass of 10.6 ± 1.5 $M_\oplus$ on a 396 ± 6 d circular orbit and a likely more massive Neptunian exoplanet with a minimum mass of 24 ± 1.5 $M_\oplus$ on a 2093^{+130}_{-120} d keplerian orbit.

I. INTRODUCTION

The theory on auroral emission of stars with orbiting exoplanets has been the focus of study for many years [8], but with no observational evidence of such phenomena until a low-frequency radio emission detection consistent with an interaction of Gliese 1151 (GJ 1151) with an orbiting exoplanet was found by Vedantham et al. [20] with the LOFAR instrument. This type of emission is consistent with the well-known Jupiter-Io sub-Alfvénic interaction that has been studied by many researchers in order to understand star-planet interaction radiation by electron cyclotron maser instability [14, 19]. As argued by Vedantham et al. [20], other proposed scenarios which rely on the stand-alone emission of the star via stellar bursts fail to generate the radio power emission detected, considering that GJ 1151 is a quiescent M4.5 dwarf, with a mass of 0.170 ± 0.01 $M_\odot$ [16]. Another possibility would have been the interaction with a stellar companion, but observations with FastCam [5] already dismiss the presence of any stellar companion at a distance greater than 1 au. Following Vedantham et al. [20], the most plausible scenario for the generation of this emission seems the interaction with an Earth-like exoplanet with a 1 to 5 d period.

As a result of this announcement, many exoplanets surveys based on the radial velocity (RV) method started searching for variations in the star. The RV method consists in the detection of exoplanets by studying the Doppler-shift on the star's spectra provoked by them. Pope et al. [13] with 20 RVs from HARPS data (High Accuracy Radial velocity Planet Searcher) were not able to detect any significant signal but set an upper limit on the minimum mass of the possible planet at $M \sin i < 5.6 M_\oplus$ (being i the orbit's inclination seen from Earth). Mahadevan et al. [11] with 25 RVs extracted from near-infrared HPF (Habitable-zone Planet Finder) spectra added to the same 20 public RVs from HARPS claimed the detection of a prominent RV signal consistent with an extra-solar planet of $M \sin i = 2.5 \pm 0.5 M_\oplus$ at a 2.02 d orbit. Nevertheless, Perger et al. [12] reported that no significant signal was present combining the same data from HPF, HARPS and 70 new CARMENES (Calar Alto high-Resolution search for M dwarfs with Exo-earths with Near-infrared and optical Échelle Spectrographs) RVs extracted from the visible arm of the instrument. They set the detection limits on the data with a 99.9% significance. It corresponds to an upper limit on the minimum mass of an exoplanet at 0.7 $M_\oplus$ to 1.2 $M_\oplus$ for an orbit of 1 to 5 d, respectively. Moreover, the authors found evidence of a long-period signal >300 d. This signal is likely to be caused by a planet because the star's rotational period is T=125 ± 23 d [5] and GJ 1151 is a quiescent M dwarf with low activity so a strong stellar contribution to the RVs is not expected.

With 9 newly obtained RVs from the CARMENES instrument between February 2021 to June 2021 we try to achieve the following objectives:

1. Apply a multi-instrument fit to the data acquired with CARMENES, HARPS and HPF.

2. Establish a new upper limit on the minimum mass of the exoplanet claimed by Vedantham et al. [20].

3. Characterize the signals and planetary companions present in the data.

II. DATA

We are analyzing data of GJ 1151 coming from three different instruments: HARPS, CARMENES and HPF. The HARPS data used by Pope et al. [13], Mahadevan et al. [11] and Perger et al. [12] include 20 epochs over approximately 3 months, December 2018 to Februrary 2019. The RVs were extracted from the spectra with the HARPS-TERRA algorithm [1] following Perger et al. [12]. The HPF data used by Mahadevan et al. [11] and Perger et al. [12] include 25 epochs acquired from March 2019 to June 2020. The RVs were calculated with the SERVAL code [23]. The majority from our measurements came from the 70 epochs obtained with CARMENES by

*Electronic address: blancopozojordi@gmail.com

Perger et al. [12] with 9 new additional RVs. Therefore, we analyze 79 epochs spanned over 4 years. The CARMENES data can be divided into two blocks: 6 epochs from February 2016 to June 2016 and 72 epochs from February 2020 to June 2021, with one stand alone data point at January 2018. Therefore, there is some overlapping with the HPF data. It was also analyzed with the SERVAL code.

All the data together is presented in Fig. (2) and statistics are shown in Table I. We can see that it is unevenly sampled and extended over time so we can investigate long term variations such as the presence of a linear trend.

	HARPS	HPF	CARMENES	All
N_{obs}	20	25	79	124
rms (m/s)	2.61	4.65	3.44	3.61
δRV (m/s)	1.85	3.00	1.88	2.11
Δt (d)	3.6	19.5	25.0	13.1
T (d)	69	468	1953	1953

TABLE I: Updated table presented by Perger et al. [12] with the new CARMENES data. N_{obs} is the number of observations, rms is the root mean square of the RVs, δRV is the average uncertainty of the data, Δt is the average time sampling of the data and T is the time baseline.

III. METHODS

Exoplanet searches tend to reduce to a problem of finding a true keplerian signal in data with correlated and non-correlated noise by the instrument or the stellar host. There is also the effect of the employed frequentist search techniques such as aliasing. In order to distinguish between true and false signals, we have used several statistical methods in our research:

A. Lomb-Scargle Periodogram

The Lomb-Scargle (LS) Periodogram is an algorithm for the study of periodic signals in unevenly sampled data. Its definition and statitiscal properties were mainly discussed by Lomb [10] and Scargle [15] in order to give a powerful technique for the study of periodicities. In our research we will use the generalized Lomb-Scargle periodogram (GLS) [22] as it is a more robust method. It consists in fitting the data with a sinusoidal and a constant via the least-square methods. According to the goodness of the sinusoidal fit to our data, we assign a normalized power value at each frequency so the highest power frequencies correspond to the most prominent signals. When calculating this powers, we assign a weight on every data point according to the uncertainties on the measurements so the GLS corrects the fact that the LS method ignores non-zero mean values and errors.

Both the LS or GLS generate very noisy periodograms. In order to distinguish between true and false signals, we must know the power distribution of our data and calculate its false alarm probability (FAP). We evaluate the FAP of the signals via the bootstrap method [6, 9]. However, we are not able to distinguish between alias and true signals with the FAP. Alias will be peaks in our periodogram associated to harmonics of true signals or by the contribution of the sampling of the observations, i.e. the window function. The most prominent alias is at 1 d. It is caused by the lack of astronomical observations during daytime.

The calculations of the GLS and the FAP have been obtained with the astropy code [2].

B. Maximum Likelihood Method and Bayesian Evidence

Our main interest is applying a multi-instrumental fit to our data so we can combine all the available data in order to set an upper limit on the minimum mass of a possible exoplanet at around 1 to 5 d period. This fit is needed as the RVs from every instrument have a different defined zero of measurements. Therefore, we search for the best model to our data so we can find the relative RV offsets between the different RV sets. The Maximum Likelihood Method (MLM) [3] is based on constructing a Maximum Likelihood Estimator (MLE) which the best fitting model will maximize. The MLE is defined as

$$\ln(\mathcal{L}) = -\frac{\widetilde{\mathcal{X}}}{2\kappa} - \frac{N\ln\kappa}{2} - \frac{\langle\ln\omega\rangle}{2} + C \tag{1}$$

where $\mathcal{L}$ is the MLE, $\widetilde{\mathcal{X}} = \kappa\mathcal{X} = \langle\omega(v-\nu)^2\rangle$ being κ the error variance for the unit weight, v the RVs measurements, ω are the weights of every data point and $\nu = \nu(t, \boldsymbol{\theta})$ (2) is the model we are fitting depending on $\boldsymbol{\theta}$ which is the vector that contains the model parameters. In this model we incorporate linear trends and keplerian signals by numerically solving the Kepler problem (5, 6).

$$\nu = \sum_j \mu_j + \gamma(t-t_0) + \sum_j K_j(\cos(\omega_j + f_j) + e_j\cos(\omega_j)) \tag{2}$$

$$K = \frac{m_2}{m_1+m_2}\frac{2\pi a\sin i}{T\sqrt{1-e^2}} \tag{3}$$

$$T^2 = \frac{4\pi^2}{G(m_1+m_2)}a^3 \tag{4}$$

$$M = E - e\sin E \tag{5}$$

$$f = 2\tan^{-1}\left(\sqrt{\frac{1+e}{1-e}}tan\frac{E}{2}\right) \tag{6}$$

The model parameters can be divided into:

1. Physical parameters:
   (a) γ: slope of the linear trend.
   (b) t_0: time of transit.
   (c) f: angle.
   (d) K: semi-amplitude of the orbit.
   (e) a: semi-major axis.
   (f) m_1: mass of the star.
   (g) m_2: mass of the exoplanet.
   (h) i: orbit inclination.
   (i) E: eccentric anomaly.
   (j) M: mean anomaly.
2. Instrument parameters:
   (a) μ: RV offsets of the RVs of different instruments.
   (b) σ: jitter term of RVs of different instruments. These are additive errors particular to each instrument so we can adjust the relative importance of every dataset in our fitted model.

We fit different models of increasing complexity to our data. Starting from just a simple linear trend to the combination of trend and multi-planetary signals. When trying to compare models with different number of parameters we use Bayesian theory in order to obtain the best fit model. The Bayesian evidence (Z) [18] is the integral of the MLE over the prior volume which the best-fitting model maximizes. The prior volume is the parameter space over which we evaluate the models. Z allows us to compare models where we have adjusted a different number of parameters as it penalizes more complex models. Calculating the Bayes factor, defined as the difference between the logarithm of the Bayesian evidence (lnZ) of the models we are comparing, and relating this value to the Jeffreys scale [18], we favor a more complex model when it improves lnZ>2.5, indicating a moderate improvement.

In our study we have used the juliet code [7]. This is an open-source python code for the fitting of photometric and RV data via the MLM combined with Bayes theory. Juliet is able to calculate Z in wide volume priors and obtain the posterior distribution of the parameters of the model fitted in just a few minutes. It does that by taking advantage of Monte-Carlo sampling methods. They allow to effectively calculate the evidence by shrinking the volume prior by evaluating new samples of increasing likelihood at each iteration until the stopping criteria defined by the user is met. The samples are the points over we evaluate the integral. In particular juliet can evaluate this integral by the classical Nested Sampling method or by the Dynamic Nested Sampling. The last one is implemented by dynesty [17] and it is the one used it in our study. The main difference between the two methods is that the number of samples over which dynesty evaluates the evidence is not previously defined and will be modified across iterations, exploring more effectively the volume prior.

IV. RESULTS

Using the statistical tools presented in the previous section, we look for periodicities in our data in order to find the best multi-instrumental fit. We aim to improve the detection limits derived by Perger et al. [12] so we can update the upper limit on the minimum mass of an exoplanet with a 1 to 5 d orbit.

A. Model discussion

In order to combine the three data sets we search for the best fitting model with juliet. The previously known feature in our data is the existence of a signal > 300 d and a linear trend [12]. This linear trend could be an even longer-period exoplanet with a period similar to our time baseline of ~ 6 y. Therefore, we set restrictive priors over the short-period exoplanet and let the other priors wide. In Table II we show the obtained lnZ for the different models. Following the criteria established by the Jeffrey scale (lnZ>2.5) we find that the best model is the 2 planets model (lnZ=-304.6 $\pm$ 0.4) while also setting the shorter period exoplanet to e=0. From all models with -304.6 > lnZ > -302.1, this is the model with the lowest complexity.

B. 2 planets model

As we see from the obtained parameters (Table III), the best model consists of two Neptune-type exoplanets with orbits of 396 ± 6 d and 2093^{+130}_{-120} d (Fig. 2). The first Neptune, with a minimum mass of 10.6 ± 1.5 $M_\oplus$ and semi-major axis 0.584 ± 0.006 au (Eq. 3 and 4), is present in all the models which incorporate planetary companions. This give us confidence on the existence of this planet. Although we have certain evidence of its low eccentricity, we are not able to determine it with precision because the observations have not equally explored all phases of the orbit (Fig. 1). The second exoplanet, with a minimum mass of 24 ± 9 $M_\oplus$ and semi-major axis 1.77 ± 0.07 au, its existence it is not so certain. An exoplanet with such long orbit, barely over the time baseline, can be confused with a linear trend. More observations are needed in order to confirm or propose another scenario.

After applying the RV offsets and jitter terms obtained with the best fitting model, we subtract the 2 planets signal from our data so we can obtain the residuals. These residuals do not include any significant signal (FAP<0.1%) into our periodogram (Fig. 3) so it can be considered that all remaining data consists of noise.

Model	lnZ
No Signal	-344.7 ± 0.3
Linear Trend	-334.0 ± 0.3
1 Planet e=0	-319.0 ± 0.4
1 Planet	-318.1 ± 0.4
Linear Trend+1 Planet e=0	-308.1 ± 0.4
Linear Trend+1 Planet	-309.8 ± 0.4
2 Planets e_1=0	-304.6 ± 0.4
2 Planets	-307.2 ± 0.4
Linear Trend+2 Planets e_1=0	-303.2 ± 0.4
Linear Trend+2 Planets	-303.5 ± 0.4
3 planet e_1=0	-302.9 ± 0.4
3 planet	-305.1 ± 0.5
Linear Trend+3 Planets	-304.8 ± 0.5

TABLE II: Logarithm of the bayesian evidence with its error for each model.

Parameter	Median	Priors
$P_1(d)$	396^{+6}_{-6}	U(350,450)
$t_{01}(d)$	2457389^{+22}_{-24}	U(2457219.67815, 2457619.67815)
$K_1(m/s)$	$3.0^{+0.4}_{-0.3}$	U(0,10)
ω_1	230^{+80}_{-113}	U(0,360)
$P_2(d)$	2093^{+130}_{-120}	U(1500,2500)
$t_{02}(d)$	2457366^{+98}_{-90}	U(2457219.67815, 2457619.67815)
$K_2(m/s)$	$4.1^{+1.6}_{-0.9}$	U(0,10)
e_2	$0.33^{+0.19}_{-0.15}$	U(0,1)
ω_2	175^{+38}_{-57}	U(0,360)
$\mu_{CARMENES}(m/s)$	$-1.7^{+0.5}_{-0.5}$	U(-10,10)
$\mu_{HARPS}(m/s)$	$-5.0^{+1.1}_{-1.2}$	U(-10,10)
$\mu_{HPF}(m/s)$	$-3.3^{+0.9}_{-1.0}$	U(-10,10)
$\sigma_{CARMENES}(m/s)$	$0.5^{+0.3}_{-0.3}$	U(0,10)
$\sigma_{HARPS}(m/s)$	$2.1^{+0.6}_{-0.5}$	U(0,10)
$\sigma_{HPF}(m/s)$	$2.6^{+0.8}_{-0.9}$	U(0,10)

TABLE III: Parameters from Eq. 2-6 for the 2 planets model with the assumed priors.

C. Detection limits

In order to derive the detection limits of a short-period exoplanet, we follow the method applied by Zechmeister et al. [21] and Bonfils et al. [4]. After no significant signal was found in the period range of interest (1 to 5 d), setting as a criteria no signal with FAP<0.1%, all remaining data is noise. Then, we inject artificial planet orbits with the same time sampling of our data at different 12 equi-spaced phases. Starting with the semi-amplitude of the most prominent signal within the range of study, we look for the minimum semi-amplitude that provides a significant signal at the frequency that we have injected. Therefore, we see the upper limit on the minimum mass an exoplanet hidden by our noisy data could have. We inject planets from 0.2 to 0.98 d^{-1} with 390 equi-spaced steps of 1/500 d^{-1}. We do not evaluate for 1 d because of the 1 d alias. We obtain a detection limit by imposing the FAP threshold on the 12 phases. The detection limit calculated as a semi-amplitude is K=1.9 ± 0.5 m/s. This translates into a minimum mass of 0.9 $M_\oplus$ and 1.6 $M_\oplus$ for the 1.02 d and 5 d period, respectively (Fig. 4). Therefore, we are not able to discard the existence of the terrestrial exoplanet proposed by Vedantham et al. [20].

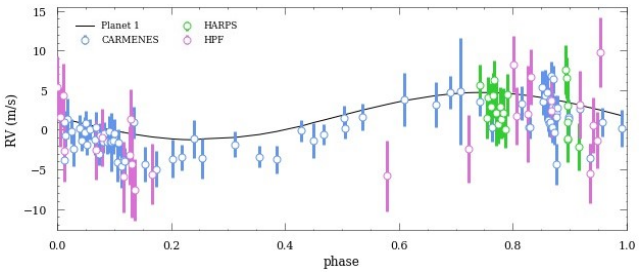

FIG. 1: Phase folded representation of the data for the 396±6 d period exoplanet with the 2093^{+130}_{-120} d exoplanet subtracted. Half of the phase is not well explored.

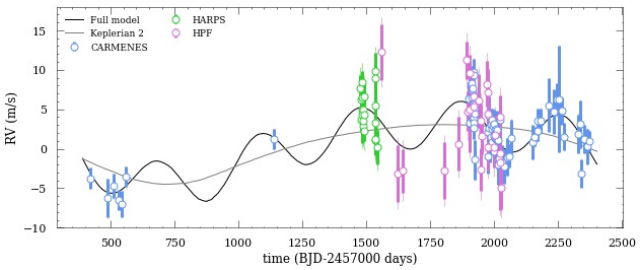

FIG. 2: Final fit for the combined data modelled as a 2 planets signal. The jitter term is added as a thinner error bar.

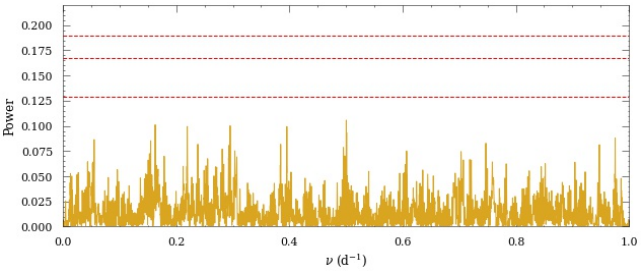

FIG. 3: LS periodogram of the residuals after subtracting the 2 planets signal. The horizontal lines represent (from top to bottom) the 0.1%, 1%, 10% FAP.

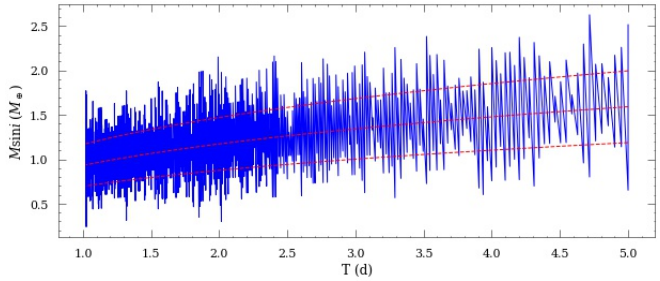

FIG. 4: Upper limit on the minimum mass of a planet orbiting with a 1.02 to 5 d period around GJ 1151. The red lines represent the mean value and its 1-σ error.

V. CONCLUSION

After Vedantham et al. [20] reported the detection of a radio emission which had most likely been generated by the interaction of an Earth-like planet with its star, many exoplanet surveys put their focus on detecting such planet. With the data gathered by HARPS, HPF and CARMENES we perform a multi-instrument fit. Then, we subtract the best-fitting model so we can calculate our detection limits: K=1.9 ± 0.5 m/s. With Eq. 3 we convert this into an upper limit on the minimum mass of a possible companion at 0.9 $M_\oplus$ to 1.6 $M_\oplus$ for a 1.02 d to 5 d orbit. This constraint does not rule out the scenario proposed by Vedantham et al. [20], as an Earth-type exoplanet would still be able to produce the radio emission detected by LOFAR.

We also manage to find evidence of a Neptune with a minimum mass of 10.6 ± 1.5 $M_\oplus$ and with an orbit of 396 ± 6 d and a likely more massive companion at 2093^{+130}_{-120} d and 24 ± 1.5 $M_\oplus$. Such long orbits would not be able to produce a radio emission by the sub-Alfvénic interaction with GJ 1151 as proposed by Vedantham et al. [20]. There is a strong evidence for this 2 Neptunes model as it improves the lnZ for lnZ > 40 compared to the no signal model (Table II).

For further research we expect to better constrain the eccentricity of the first exoplanet as we better explore regions of the phase with less observations (0.3 < phase < 0.7). This window of less explored phases of the orbit will correspond to October 2021 to March 2022. Therefore, in the next CARMENES season of observations we will be able to improve the fit in our data. Moreover, with more observations we aim to gather more information about the nature of the longer keplerian signal.

Acknowledgments

I would like to thank Dr. Manuel Perger for his invaluable guidance and knowledge during this project. Also Dr. Carme Jordi for her advice and help. I am also grateful for the unconditional support my family and friends have given me during all these years.

[1] Anglada-Escudé, G. & Butler, R. P. 2012, The Astrophysical Journal Supplement Series, 200, 15
[2] Astropy Collaboration, Robitaille, T. P., Tollerud, E. J., et al. 2013, Astronomy and Astrophysics, 558, A33
[3] Baluev, R. V. 2009, Monthly Notices of the Royal Astronomical Society, 393, 969
[4] Bonfils, X., Delfosse, X., Udry, S., et al. 2013, Astronomy and Astrophysics, 549, A109
[5] Díez Alonso, E., Caballero, J. A., Montes, D., et al. 2019, Astronomy and Astrophysics, 621, A126
[6] Efron, B. 1979, The Annals of Statistics, 7, 1
[7] Espinoza, N., Kossakowski, D., & Brahm, R. 2019, Monthly Notices of the Royal Astronomical Society, 490, 2262
[8] Farrell, W. M., Desch, M. D., & Zarka, P. 1999, Journal of Geophysical Research: Planets, 104, 14025
[9] Ivezić, Ž., Connelly, A. J., VanderPlas, J. T., & Gray, A. 2014, Statistics, Data Mining, and Machine Learning in Astronomy
[10] Lomb, N. R. 1976, Astrophysics and Space Science, 39, 447
[11] Mahadevan, S., Stefánsson, G., Robertson, P., et al. 2021, arXiv e-prints, arXiv:2102.02233
[12] Perger, M., Ribas, I., Anglada-Escudé, G., et al. 2021, Astronomy & Astrophysics, 649, L12
[13] Pope, B. J. S., Bedell, M., Callingham, J. R., et al. 2020, , 890, L19
[14] Saur, J., Neubauer, F., Connerney, J., Zarka, P., & Kivelson, M. 2004, Jupiter. The Planet, Satellites and Magnetosphere
[15] Scargle, J. D. 1982, Astrophys. J. , 263, 835
[16] Schweitzer, A., Passegger, V., Cifuentes, C., et al. 2019, Astronomy & Astrophysics, 625, A68
[17] Speagle, J. S. 2020, Monthly Notices of the Royal Astronomical Society, 493, 3132
[18] Trotta, R. 2008, Contemporary Physics, 49, 71
[19] Turnpenney, S., Nichols, J. D., Wynn, G. A., & Burleigh, M. R. 2018, The Astrophysical Journal, 854, 72
[20] Vedantham, H. K., Callingham, J. R., Shimwell, T. W., et al. 2020, Nature Astronomy, 4, 577
[21] Zechmeister, M., Kürster, M., & Endl, M. 2009, Astronomy and Astrophysics, 505, 859
[22] Zechmeister, M. & Kürster, M. 2009, Astronomy Astrophysics, 496, 577–584
[23] Zechmeister, M., Reiners, A., Amado, P. J., et al. 2018, Astronomy and Astrophysics, 609, A12